

93 **Figure S1. Identification and characterization of *Col1a2^{+/G610C}.ApoE^{-/-}* mice (*OI.ApoE^{-/-}*),**

94 *hSOST^{ki}.Col1a2^{+/G610C}.ApoE^{-/-}* mice (*hSOST^{ki}.OI.ApoE^{-/-}*), *Δloop3-hSOST^{ki}.Col1a2^{+/G610C}.ApoE^{-/-}* mice (*Δloop3-*
95 *hSOST^{ki}.OI.ApoE^{-/-}*), *hSOST^{ki}.Col1a2^{+/G610C}* mice (*hSOST^{ki}.OI*) and *Δloop3-hSOST^{ki}.Col1a2^{+/G610C}* mice (*Δloop3-*
96 *hSOST^{ki}.OI*), respectively. **(A)** Representative agarose gel electrophoretic images for PCR genotyping samples from
97 *Col1a2^{+/G610C}.ApoE^{-/-}* mice. **(B)** Representative agarose gel electrophoretic images for PCR genotyping samples from
98 *hSOST^{ki}.Col1a2^{+/G610C}.ApoE^{-/-}* mice. **(C)** Representative agarose gel electrophoretic images for PCR genotyping samples from
99 *Δloop3-hSOST^{ki}.Col1a2^{+/G610C}.ApoE^{-/-}* mice. **(D)** Representative agarose gel electrophoretic images for PCR genotyping samples from
100 *hSOST^{ki}.Col1a2^{+/G610C}* mice. **(E)** Representative agarose gel electrophoretic images for PCR genotyping samples from
101 *Δloop3-hSOST^{ki}.Col1a2^{+/G610C}* mice. **(F)** Relative mRNA expression levels of human full-length sclerostin (FL hSOST) or loop3 deficient human sclerostin (Δ loop3-hSOST) in the aorta and the tibia of
102 *Col1a2^{+/G610C}.ApoE^{-/-}* mice, *hSOST^{ki}.Col1a2^{+/G610C}.ApoE^{-/-}* mice and *Δloop3-hSOST^{ki}.Col1a2^{+/G610C}.ApoE^{-/-}* mice (left),
103 as well as *Col1a2^{+/G610C}* mice, *hSOST^{ki}.Col1a2^{+/G610C}* mice and *Δloop3-hSOST^{ki}.Col1a2^{+/G610C}* mice (right), respectively,
104 detected by RT-PCR. No significant difference (ns) were found for comparison between *hSOST^{ki}.OI.ApoE^{-/-}* and *Δloop3-*
105 *hSOST^{ki}.OI.ApoE^{-/-}* groups, or *hSOST^{ki}.OI* and *Δloop3-hSOST^{ki}.OI* groups, by paired t-test. *** $P < 0.005$ and **** $P <$
106 0.0001 for a comparison vs. *OI.ApoE^{-/-}* group or *OI* group by one-way ANOVA with Tukey's post-hoc test. **(G)** Protein
107 expression levels of FL hSOST or Δ loop3-hSOST in the serum of *Col1a2^{+/G610C}.ApoE^{-/-}* mice,
108 *hSOST^{ki}.Col1a2^{+/G610C}.ApoE^{-/-}* mice and *Δloop3-hSOST^{ki}.Col1a2^{+/G610C}.ApoE^{-/-}* mice (left), as well as *Col1a2^{+/G610C}*
109 mice, *hSOST^{ki}.Col1a2^{+/G610C}* mice and *Δloop3-hSOST^{ki}.Col1a2^{+/G610C}* mice (right), respectively, detected by ELISA. ***
110 $P < 0.005$ and **** $P < 0.0001$ for a comparison vs. *OI.ApoE^{-/-}* group or *OI* group by one-way ANOVA with Tukey's post-
111 hoc test. **Note:** *ApoE^{-/-}* mutant: ~ 245 bp (*homozygous*); *Col1a2^{+/G610C}* mutant: ~ 337 bp (*homozygous*); *hSOST^{ki}*:
5'arm ~ 1465 bp, 3'arm ~ 1229 bp; *Δloop3-hSOST^{ki}*: 5'arm ~ 1465 bp, 3'arm ~ 2149 bp.

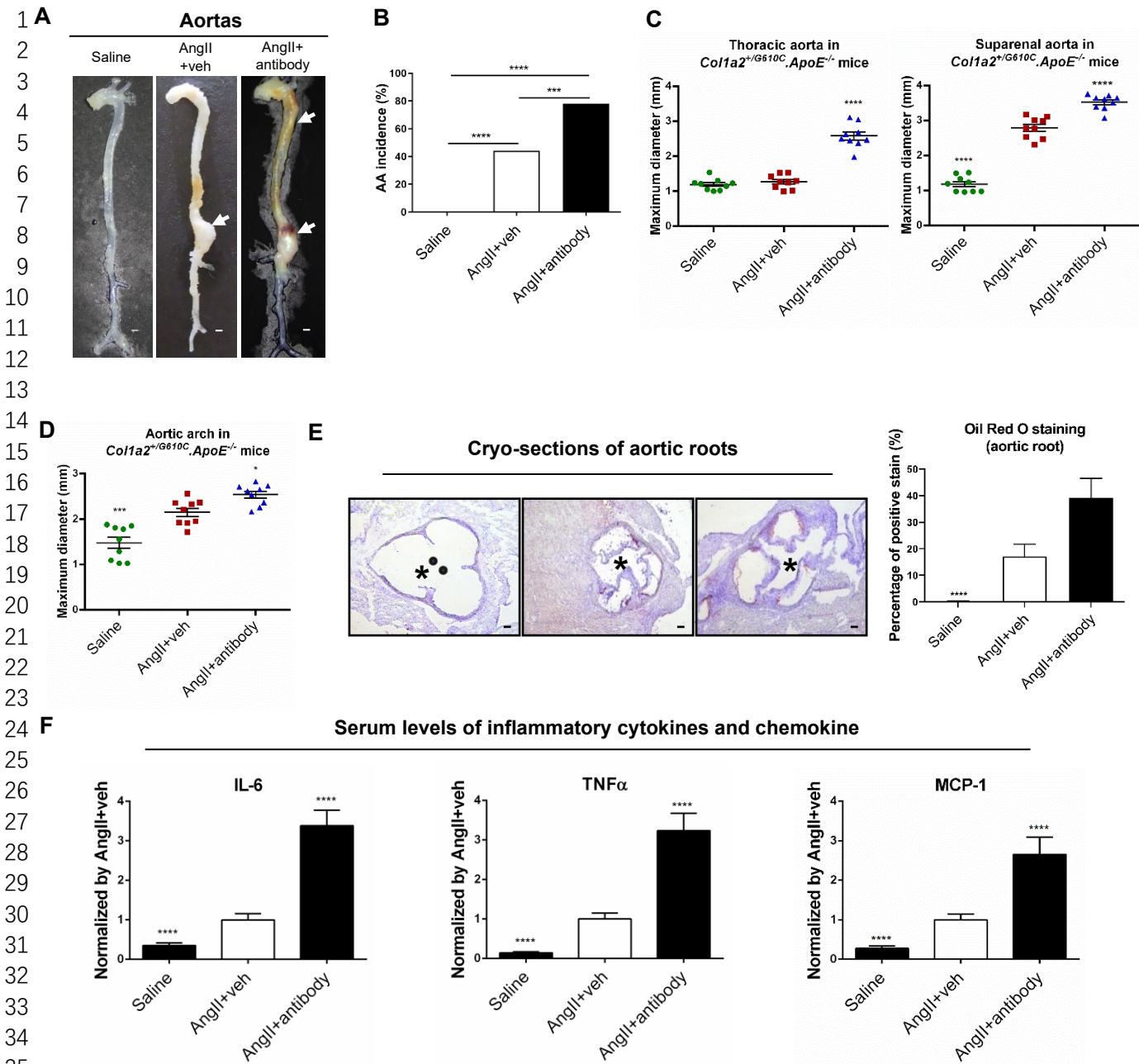


Figure S2. Therapeutic sclerostin antibody elevated serum levels of inflammatory cytokines and chemokines, aggravated AA and atherosclerosis in *Col1a2^{+/G610C}.ApoE^{-/-}* mice with AngII infusion. (A) Representative images of aortas from *Col1a2^{+/G610C}.ApoE^{-/-}* mice with AngII infusion, after administration of humanized therapeutic sclerostin antibody, respectively. The white arrows indicated the locations of AAs. Scale bars, 1 mm. (B) AA incidence of *Col1a2^{+/G610C}.ApoE^{-/-}* mice with AngII infusion. A two-sided Chi-square test was performed to determine the difference between two groups. *** $P < 0.005$ and **** $P < 0.0001$. (C) Maximum diameters of thoracic aortas (left) and suprarenal aortas (right) in *Col1a2^{+/G610C}.ApoE^{-/-}* mice with AngII infusion. (D) Maximum diameters of aortic arches in *Col1a2^{+/G610C}.ApoE^{-/-}* mice with AngII infusion. (E) Representative micrographs of cryo-sections of aortic roots from *Col1a2^{+/G610C}.ApoE^{-/-}* mice stained with Oil Red O (left). Scale bar, 100 μ m (*lumen). Quantification of positive Oil Red O stain per cryo-section (right). (F) Serum levels of inflammatory cytokines (IL-6, TNF- α) and chemokine (MCP-1) in *Col1a2^{+/G610C}.ApoE^{-/-}* mice with AngII infusion. (C-F) Data were expressed as mean \pm standard deviation ($n = 9$). * $P < 0.05$; ** $P < 0.01$; *** $P < 0.005$ and **** $P < 0.0001$ for a comparison with AngII+veh by one-way ANOVA with Tukey's post-hoc test. **Note:** AngII: Angiotensin II; IL-6: interleukin 6; TNF- α : tumor necrosis factor alpha; MCP-1: monocyte chemoattractant protein-1.

1
2
3
4
5
6
7
8
9
10
11
12
13
14
15
16
17
18
19
20
21

PK curves for aptscI56 and Apc001PE (s.c.) in $Col1a2^{+/G610C}$ mice

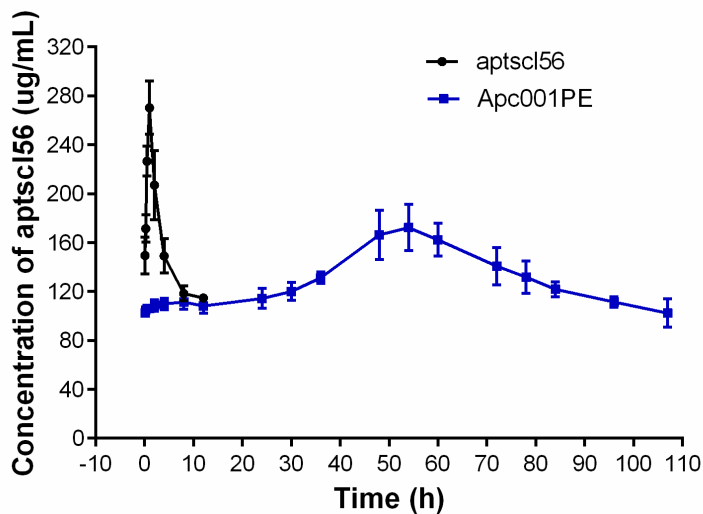
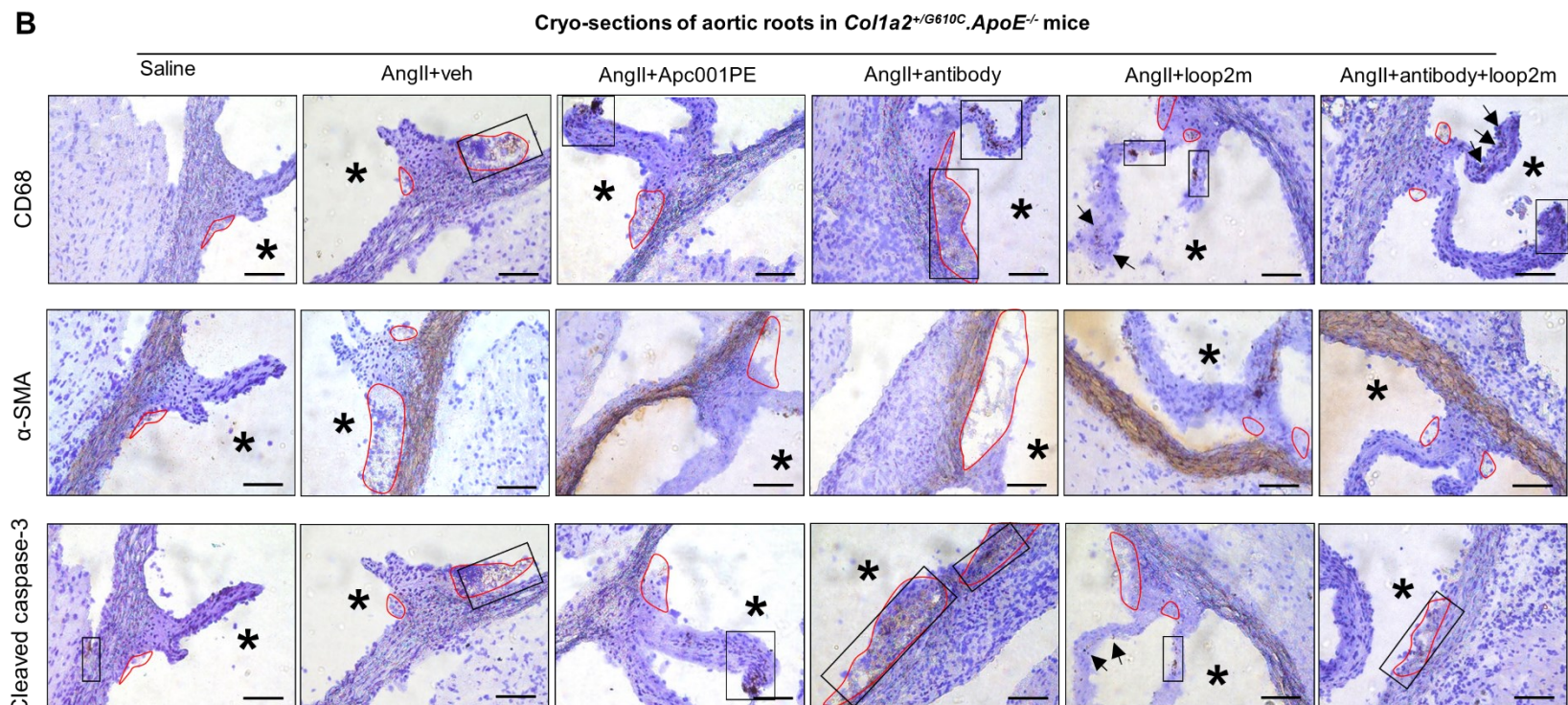
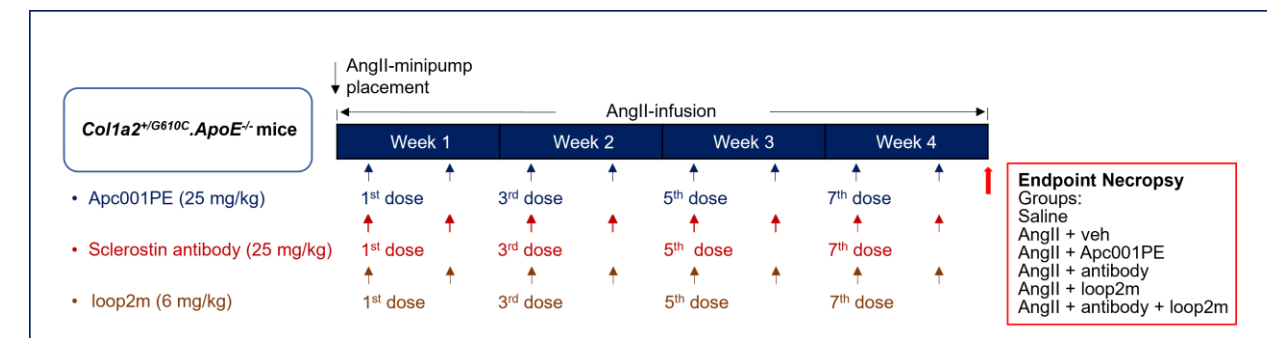


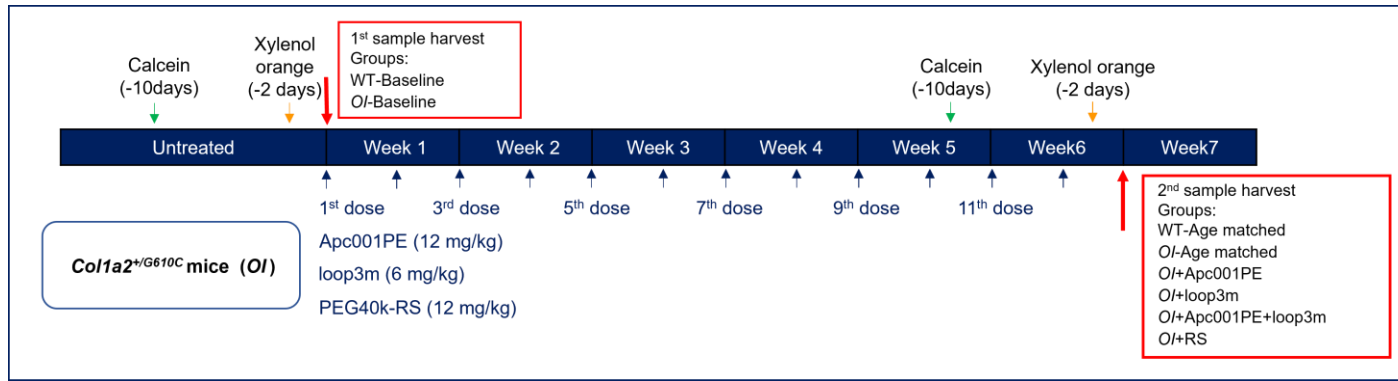
Figure S3. Pharmacokinetic analysis of aptscI56 (black) and Apc001PE (blue) after a single subcutaneous administration in $Col1a2^{+/G610C}$ mice.

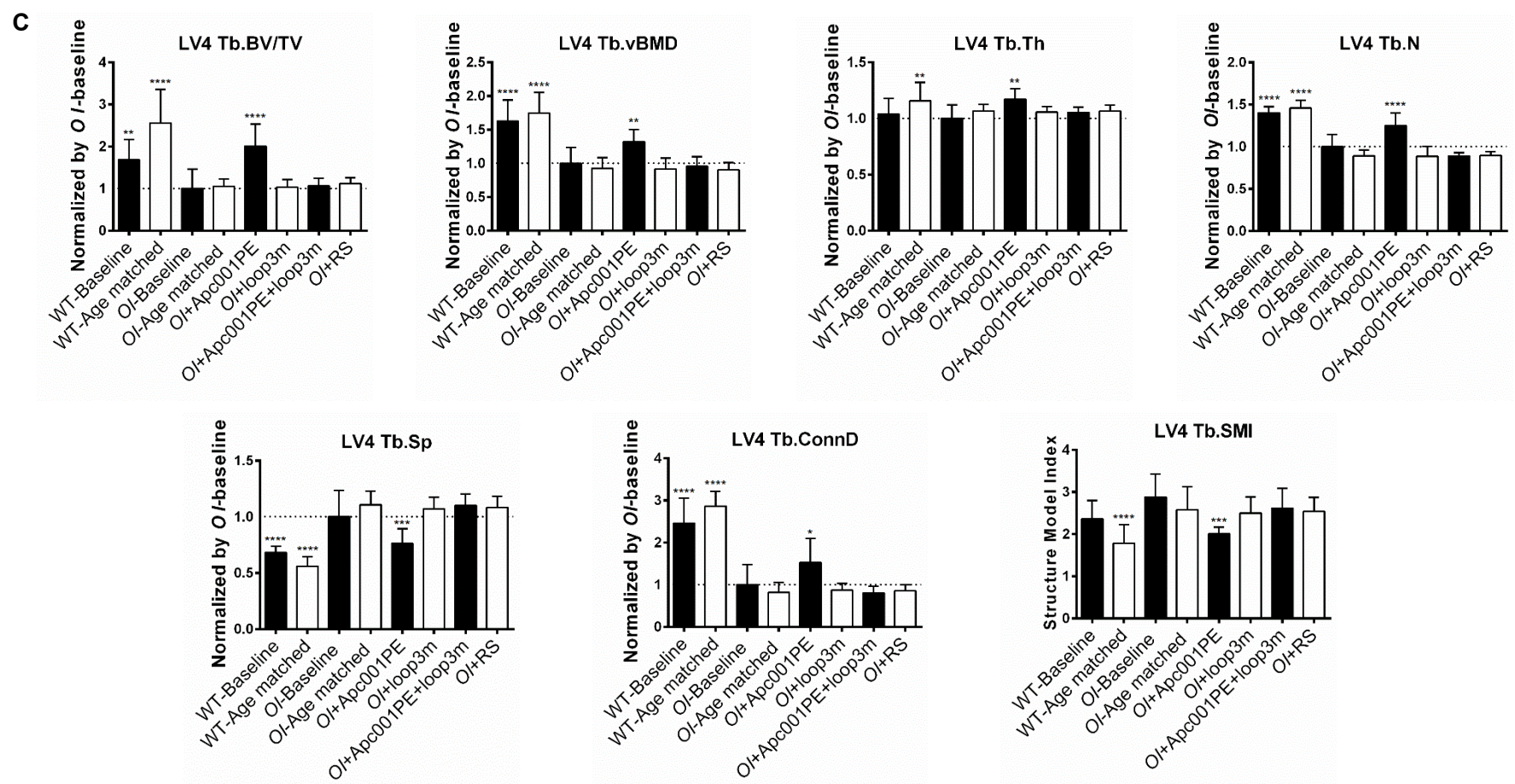
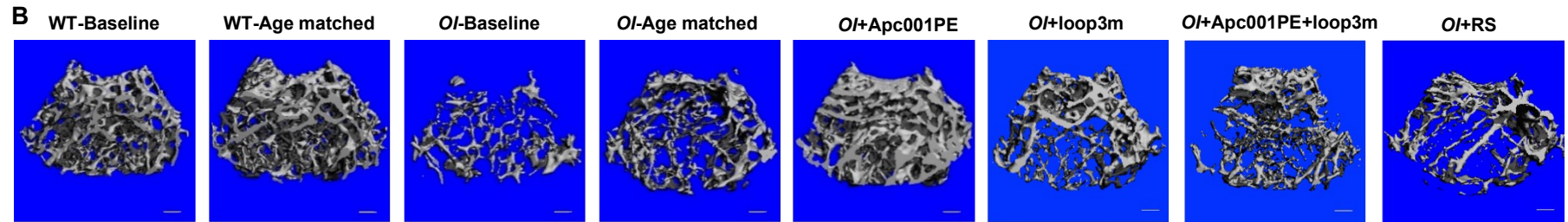
1
2
3
4
5
6
7
8
9
10
11
12
13
14
15
16
17
18
19
20
21
22
23
24
25
26
27
28
29
30
31
32
33

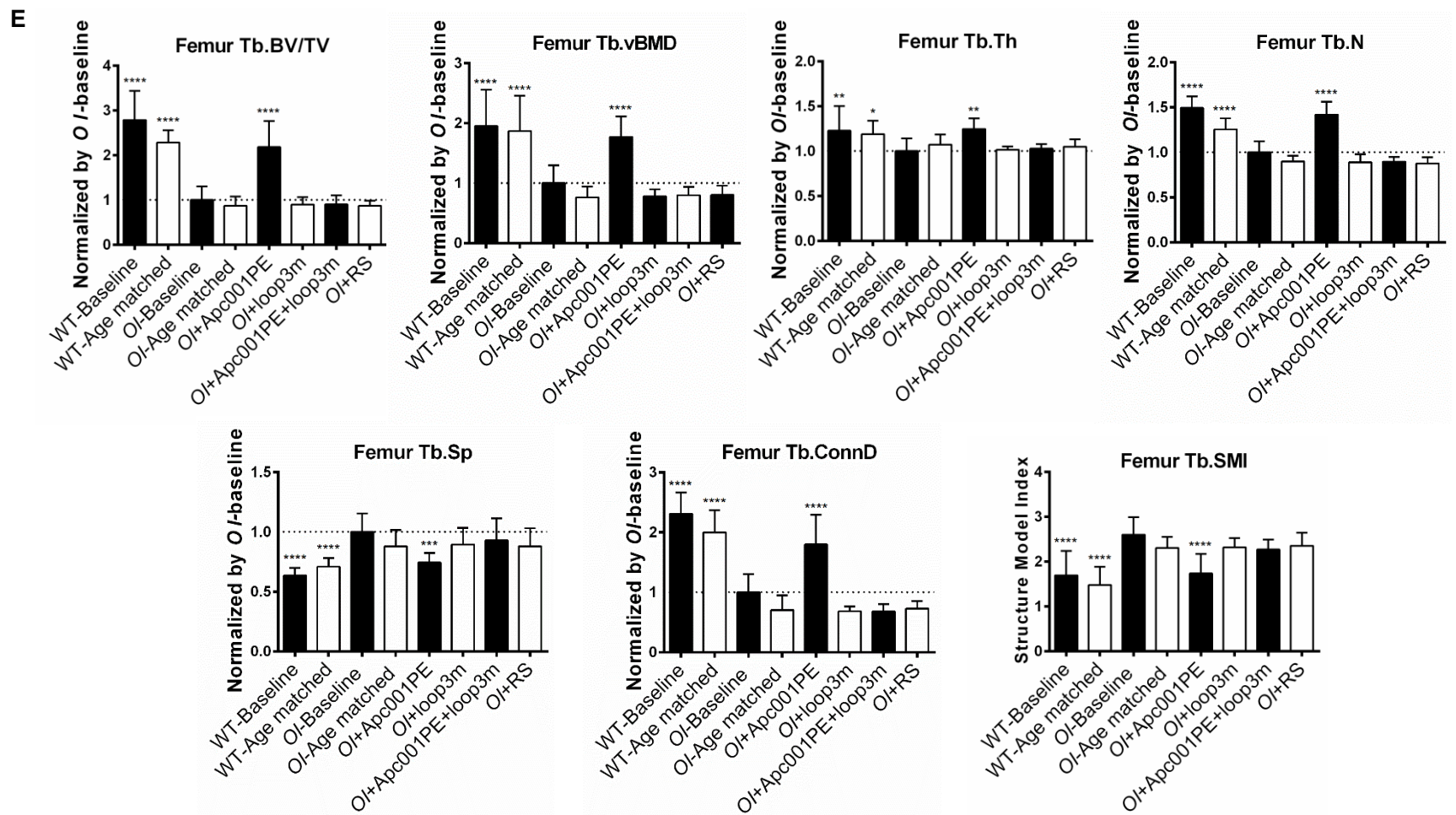
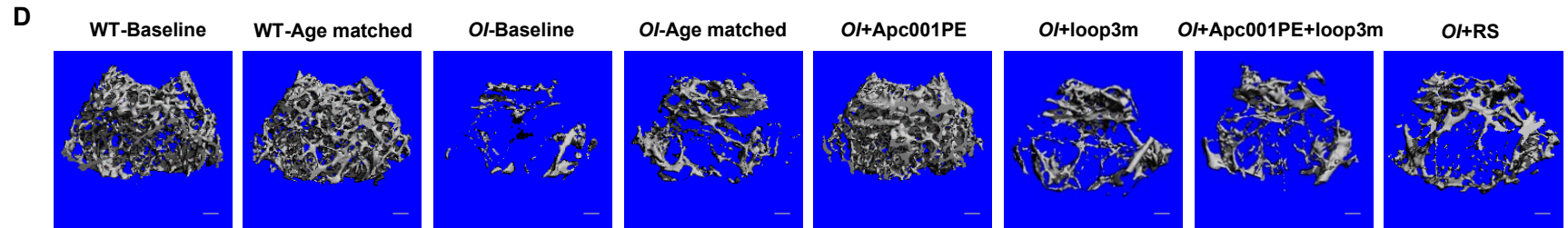
34 **Figure S4. Apc001PE had no effect on inflammatory cytokines and chemokines expression, aortic aneurysm (AA) and atherosclerosis progression in**
35 ***Col1a2^{+/G610C}.ApoE^{-/-}* mice with AngII infusion. (A)** Schematic diagram showing the experiment design of the study. Briefly, three-month-old *Col1a2^{+/G610C}.ApoE^{-/-}* mice were randomly divided into six groups: saline, AngII+veh, AngII+Apc001PE, AngII+antibody, AngII+loop2m, and AngII+antibody+loop2m ($n = 9$ for each group). For saline group, *Col1a2^{+/G610C}.ApoE^{-/-}* mice were infused with saline for four weeks. For AngII+veh, AngII+Apc001PE, AngII+antibody, AngII+loop2m, and AngII+antibody+loop2m groups, *Col1a2^{+/G610C}.ApoE^{-/-}* mice were infused with angiotensin II (AngII) for four weeks, and were subcutaneously administrated with vehicle (veh, twice per week), Apc001PE (25 mg/kg, twice per week), humanized therapeutic sclerostin antibody (25 mg/kg, twice per week), loop2m (6 mg/kg, twice per week), and therapeutic sclerostin antibody with pretreatment of loop2m (25 mg/kg + 6 mg/kg, twice per week), respectively, for four weeks during AngII infusion. (B) Representative immunohistochemistry images for the expression of CD68, α -SMA, and cleaved caspase-3 in cross cryo-sections of aortic roots from *Col1a2^{+/G610C}.ApoE^{-/-}* mice with AngII infusion (the red circles indicated the locations of atherosclerotic plaque, the black arrows and black squares indicated the locations of positive staining). Scale bars, 100 μ m (*lumen). **Note:** AngII: Angiotensin II; CD68: macrophages biomarker; α -SMA: contractile cell biomarker; Cleaved caspase-3: apoptotic cell biomarker.

1
2
3
4
5
6
7
8
9
10
11

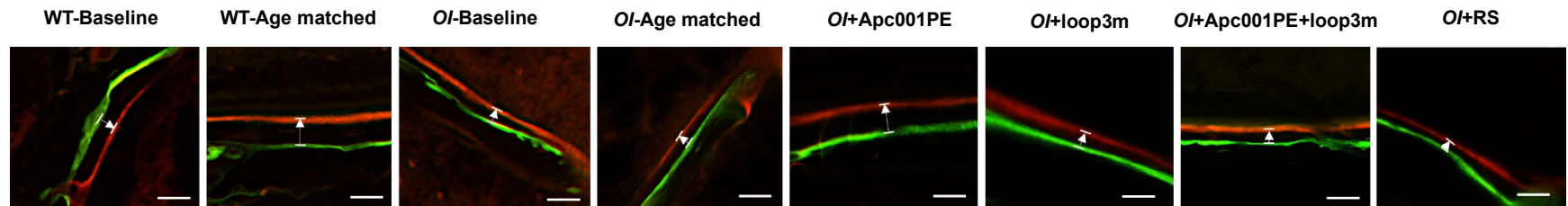
A







34

F

35

36

37

38

39

40

41

42

43

44

45

46

47

48

49

50

51

52

53

54

55

56

57

58

59

60

61

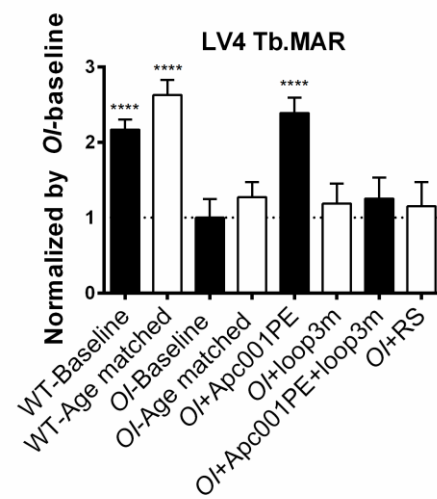
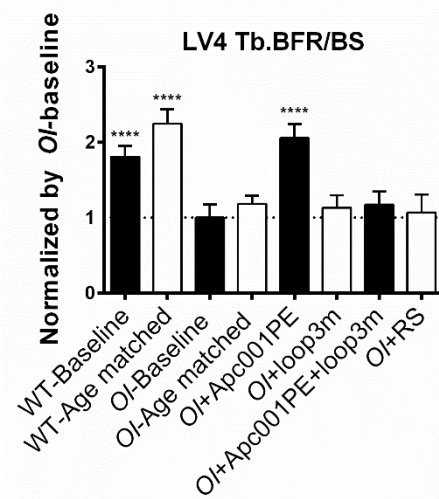
62

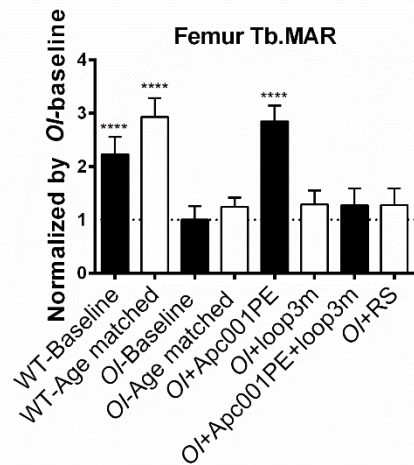
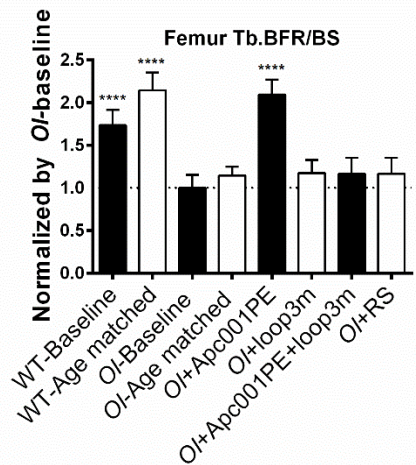
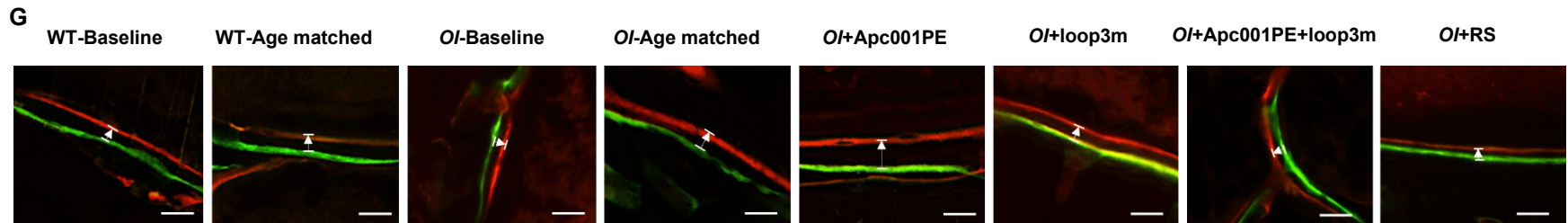
63

64

65

66





1 **Figure S5. Apc001PE promoted bone formation in *Col1a2*^{+/G610C} mice via targeting sclerostin loop3.** (A) A schematic diagram showing the experimental design
2 of the study. Briefly, ten six-week-old *Col1a2*^{+/G610C} mice (OI-Baseline) and ten six-week-old wild-type littermates (WT-Baseline) were euthanized before treatment as
3 baseline, respectively. Another ten six-week-old *Col1a2*^{+/G610C} mice (OI-Age matched) and ten six-week-old wild-type littermates (WT-Age matched) were kept
4 untreated for six weeks as the age matched groups, respectively. The remaining *Col1a2*^{+/G610C} mice were subcutaneously administrated with Apc001PE (12 mg/kg),
5 fatty acid-loop3m (loop3m, 6 mg/kg), Apc001PE+ fatty acid-loop3m (12 mg/kg + 6 mg/kg), and PEG40k-random DNA sequence (RS, 12 mg/kg), respectively, twice
6 per week for six weeks (n = 10 for each group). (B) Representative images showing three-dimensional trabecular bone architecture by micro-CT reconstruction at
7 the fourth lumbar vertebrae. Scale bars, 200 μ m. (C) Bar charts of the structural parameters of Tb.BV/TV, Tb.vBMD, Tb.Th, Tb.N, Tb.Sp, Tb.conn.D and Tb.SMI from
8 ex vivo micro-CT examination at the fourth lumbar vertebrae. (D) Representative images showing three-dimensional trabecular architecture by micro-CT
9 reconstruction at the distal femur. Scale bars, 200 μ m. (E) Bar charts of the structural parameters of Tb.BV/TV, Tb.vBMD, Tb.Th, Tb.N, Tb.Sp, Tb.conn.D and Tb.SMI
10 from ex vivo micro-CT examination at the distal femur. (F) Representative fluorescent micrographs of the trabecular bone sections showing bone formation at the
11 fourth lumbar vertebrae visualized by calcein green and xylene orange labels. Arrows indicated the spaces between calcein green and xylene orange labeling. Scale
12 bars, 40 μ m (the upper panel). Analysis of dynamic bone histomorphometric parameters of Tb.BFR/BS and Tb.MAR at the fourth lumbar vertebrae (the lower panel).
13 (G) Representative fluorescent micrographs of the trabecular bone sections showing bone formation at the distal femur visualized by calcein green and xylene orange
14 labels. Arrows indicated the spaces between calcein green and xylene orange labeling. Scale bars, 40 μ m (the upper panel). Analysis of dynamic bone
15 histomorphometric parameters of Tb.BFR/BS and Tb.MAR at the distal femur (the lower panel). **Note:** Tb.BV/TV: trabecular relative bone volume; Tb.vBMD: trabecular
16 volumetric mineral density; Tb.Th: trabecular thickness; Tb.N: trabecular number; Tb.Sp: trabecular spacing; Tb.conn.D: trabecular connect density; Tb.SMI:
trabecular structure model index; Tb.BFR/BS: trabecular bone formation rate; Tb.MAR: trabecular mineral apposition rate. Data were expressed as mean \pm standard
deviation followed by one-way ANOVA with Tukey's post-hoc test vs OI-Baseline, n = 10 per group. *P < 0.05; **P < 0.01; ***P < 0.005; ****P < 0.0001.

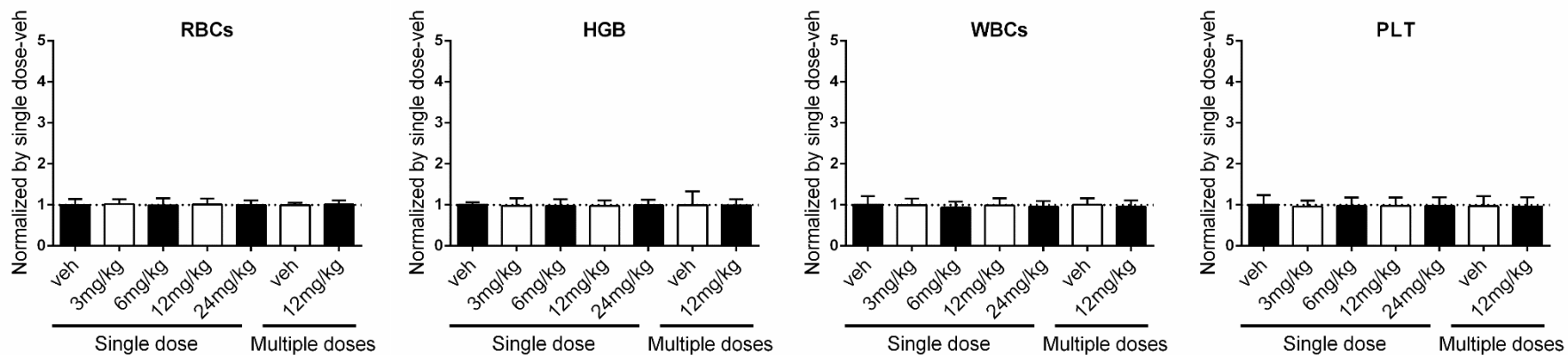
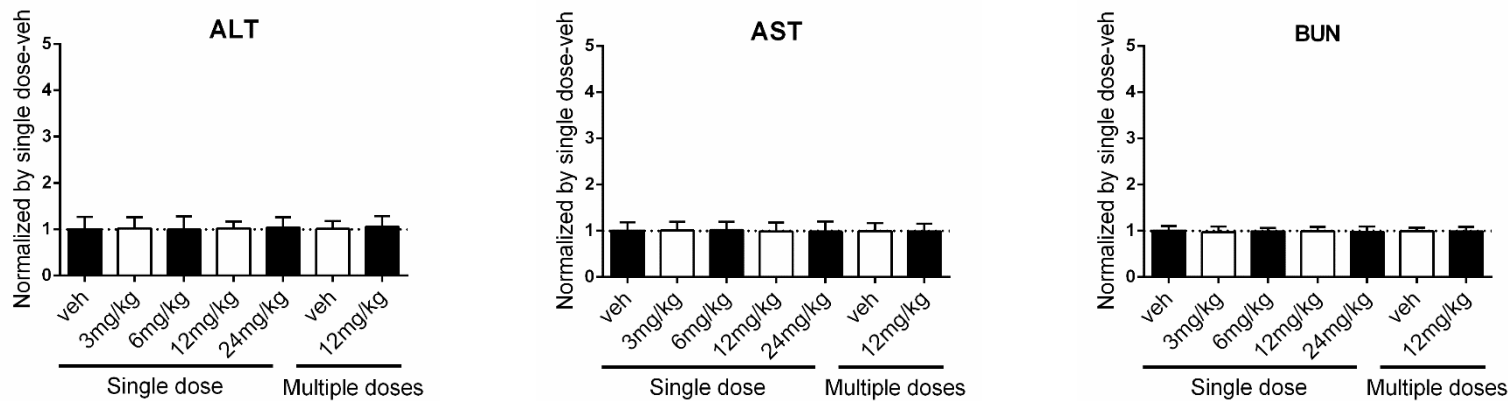
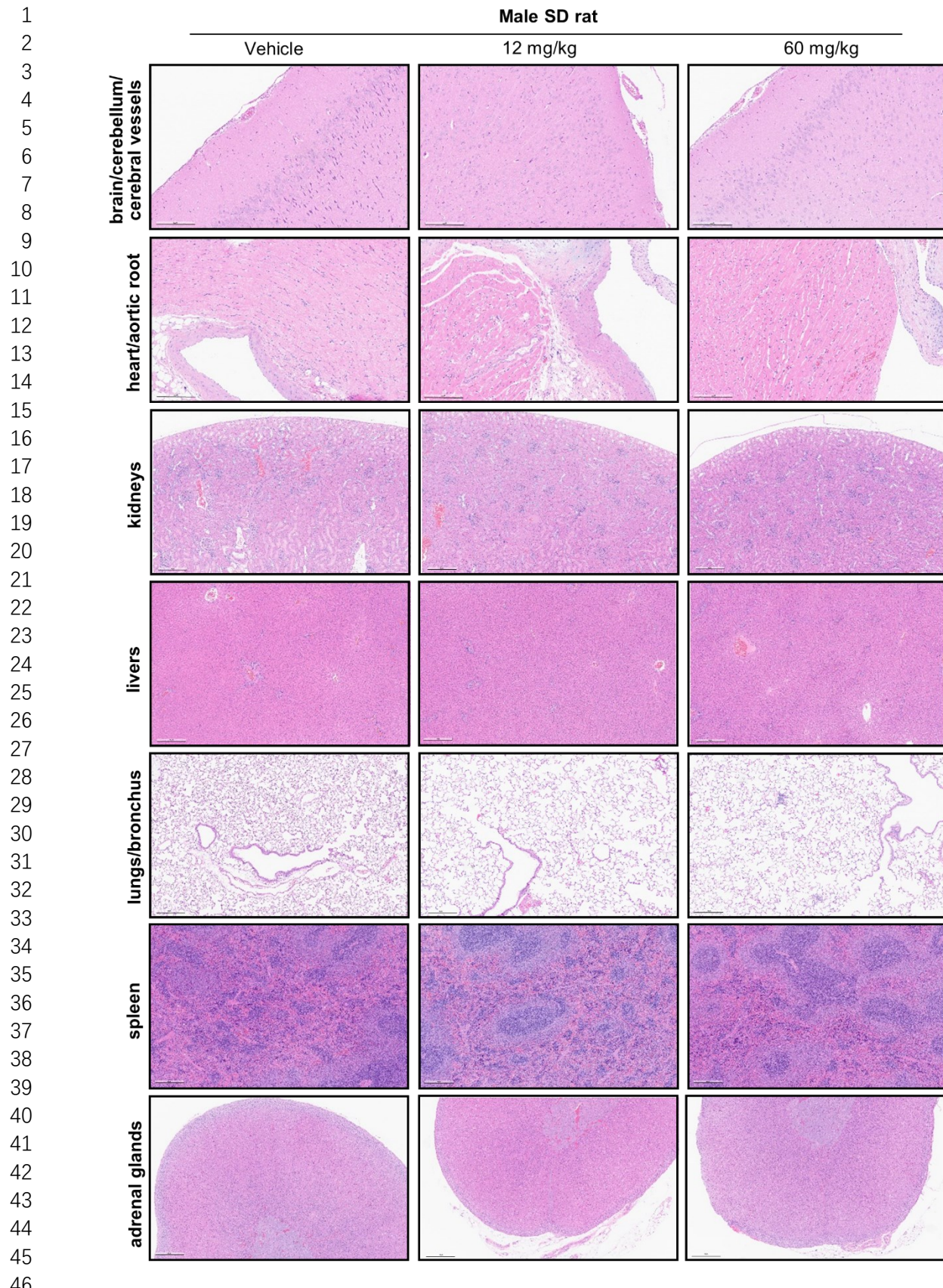
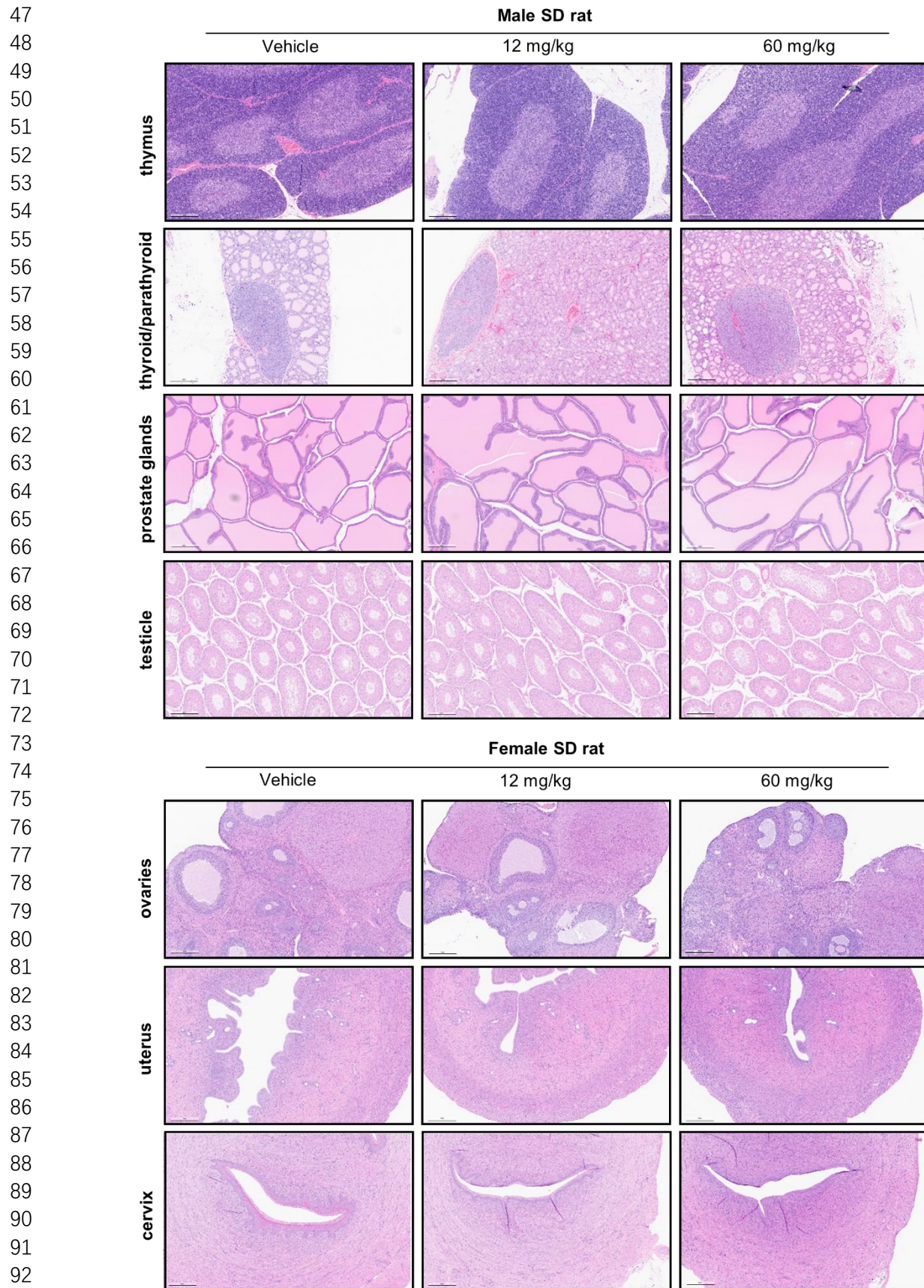


Figure S6. Serum levels of liver and kidney function indexes as well as hematologic parameters in healthy C57BL/6 mice after a single or multiple administration(s) of Apc001PE. ALT: alanine aminotransferase; AST: aspartate aminotransferase; BUN: blood urea nitrogen; RBCs: red blood cells; HGB: haemoglobin; WBCs: white blood cells; PLTs: platelets. Data were expressed as mean \pm standard deviation followed by one-way ANOVA with Tukey's post-hoc test, n = 10 per group.





93 **Figure S7. The sclerostin loop3-specific aptamer did not induce lesions and pathological changes in vital**
94 **organs of healthy SD rats.** Histopathological images of the paraffin sections of the vital organs including
95 brain/cerebellum/cerebral vessels, heart/aortic root, kidneys, livers, lungs/bronchus, spleen, adrenal glands, thymus,
96 thyroid/parathyroid, prostate glands, testicle, ovaries, and uterus/cervix in healthy SD rats, after administration of the
97 sclerostin loop3-specific aptamer at the dosage of 12 mg/kg and 60 mg/kg, respectively, twice per week for six weeks.
98 Differences among three groups were not found ($n = 5$). Scale bar for brain/cerebellum/cerebral vessels and heart/aortic
99 root: 200 μm . Scale bar for the other organs: 300 μm .

1
2
3

Table S1. Pharmacokinetic parameters of aptscI56 and Apc001PE after a single subcutaneous administration in *Col1a2*^{+G610C} mice.

Parameter	Mean value	
	aptscl56	Apc001PE
AUC _{0-t} (mg/L*h)	1336.928	13604.239
AUC _{0-∞} (mg/L*h)	2682.447	28253.472
T _{1/2} (h)	0.8	57.798
CL/F (L/h/kg)	0.002	0
V/F (L/kg)	0.015	0.018
T _{max} (h)	1	54

4
5